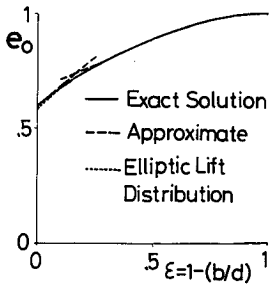

Fig. 2 Open-tunnel case span efficiency factor e_0 vs ϵ.

A following open-tunnel case span efficiency factor in the minimum induced drag is obtained:

$$e_0 = \frac{8}{\pi^2}\left[\frac{k-1}{2k^2}(1-k^2)K^2 + \frac{1-k}{k^2}KE - \frac{E^2}{2k^2}\right] + \frac{1}{k} \qquad (6)$$

When b/d reaches zero, the approximate solution of e_0 is

$$e_0\Big|_{b/d\to 0} = 1 - \frac{k}{2} + \frac{k^2}{4} - \frac{7}{32}k^3 + \frac{5}{32}k^4 + \mathcal{O}(k^5)$$

If b/d reaches unity, the approximate solution of e_0 is

$$e_0\Big|_{b/d\to 1} = 1 - (4/\pi^2) + 2\epsilon[1 - (4/\pi^2)]$$

The relation of the open-tunnel case span efficiency factor e_0 to ϵ is examined by high-speed digital computer and shown in Fig. 2.

Conclusions

The closed forms of both the spanwise optimum lift distribution and the minimum induced drag in the closed-tunnel case are obtained, and the results are coincident with those of our previous paper. Open-tunnel case explicit expressions of both the spanwise optimum lift distribution and the minimum induced drag are obtained.

Appendix: Elliptic Spanwise Lift Distribution Wing in Closed or Open Wind Tunnel

The span efficiency factor of a wing in a circular closed or open tunnel e_{ellipt} is as follows[4]:

$$e_{\text{ellipt}} = \frac{1}{1 \mp [4/(\pi k)]\,[(\pi/2) - E]} \qquad (A1)$$

where the $-$ sign of the double sign $\mp$ indicates the closed-tunnel case and the $+$ sign indicates the open-tunnel case.

The asymptotic solutions for $b/d \to 0$ are

$$e_{\text{ellipt}} = 1 \pm \frac{k}{2} + \frac{k^2}{4} \pm \frac{7}{32}k^3 + \frac{5}{32}k^4 + \mathcal{O}(k^5) \qquad (A2)$$

where the $+$ sign of each double sign $\pm$ indicates the closed-tunnel case and the $-$ sign indicates the open-tunnel case.

The limiting values at $b/d \to 1$ are

$$e_{\text{ellipt}_{b/d=1}} = \frac{1}{1 \mp [2 - (4/\pi)]} \qquad (A3)$$

where the $-$ sign of the double sign $\mp$ indicates the closed-tunnel case and the $+$ sign indicates the open-tunnel case.

Acknowledgment

The author would like to express his appreciation to S. Ando.

References

[1]Ando, S., and Yamamoto, Y., "Induced Drag of a Straight Wing in a Wind Tunnel of Circular Cross Section," *Ingenieur Archiv*, Bd. 45, H. 3, 1976, pp. 161-170.

[2]Bisplinghoff, R. L., Ashely, H., and Halfman, R. L., *Aeroelasticity*, Addison-Wesley, Cambridge, MA, 1955, p. 217.

[3]Rosenhead, L., "The Effect of Wind Tunnel Interference on the Characteristics of an Aerofoil," *Proceedings of the Royal Society of London, Series A*, Vol. 129, Nov. 1930, pp. 135-145.

[4]Moriya, T., *Introductions to Aerodynamnics*, in Japanese, Baifukan, Tokyo, 1959, pp. 233-238.

[5]Millikan, C. B., "On the Lift Distribution for a Wing of Arbitrary Plane Form in a Circular Wind Tunnel," *Transactions of the ASME, Journal of Applied Mechanics*, APM-54-19, 1932, pp. 197-203.

[6]Rae, W. H., Jr., and Pope, A., *Low-Speed Wind Tunnel Testing*, 2nd ed., Wiley, New York, 1984, pp. 376-383.

[7]Byrd, P. F., and Friedman, M. D., *Handbook of Elliptic Integrals for Engineers and Scientists*, 2nd ed., Springer-Verlag, Berlin, 1971.

Qualitative Model for Visualizing Shock Shapes

Masatomi Nishio*
Fukuyama University, Fukuyama 729, Japan

I. Introduction

THE visualization of three-dimensional shock shapes using electric discharge was previously attempted.[1] However, we did not know reasonable theory of the visualization. Therefore, it has been difficult to select suitable experimental conditions. Consequently, the visualization of shock shapes has been difficult and they have not been visualized very successfully. A qualitative theory of the visualization has now been established by considering the relation among the radiation intensity from the electric discharge, the excitation function vs electron energies, and the gas molecular number density. Applying this qualitative theory of the visualization, it was found that there exists the most suitable experimental condition. Utilizing this knowledge, it has become easy to visualize three-dimensional shock shapes.

II. Visualizing Principle

In general, excitation functions rise according to the increase of electron energies and, once they have reached their maximums, decline according to the increase of electron energies. As mentioned by Nasser,[2] the decline in all types of excitation functions after reaching the maximums can be explained purely qualitatively by considering the actual collision process that can be visualized by considering the interaction of the electromagnetic fields of the two colliding particles. When the oncoming particle is a fast electron "wave," the period of interaction of the fields of the waves of both particles become very short. The amount of kinetic energy and momentum transferred from the electron to the molecule also decreases. Hence, if the electron is too fast no "collision" takes place, as no appreciable interaction of fields is effective in the short time.

Radiation intensity I from an electric discharge is proportional to the product of the excitation function F and the gas molecular number density N. Because the excited molecule's electron, upon resuming stability, discharges light in an amount equal to its excitation energy, and because the number

Received Sept. 17, 1991; revision received Jan. 22, 1992; accepted for publication Feb. 10, 1992.

*Associate Professor, Department of Mechanical Engineering. Member AIAA.

of discharges of such light is proportional to the molecular number density, the following equation is established:

$$I \propto F \times N \tag{1}$$

Therefore, if the gas molecule type is the same, the curve (I-curve) can be drawn as shown in Fig. 1, with the electron energy as the abscissa and the radiation intensity as the ordinate, and the molecular number density N as the parameter. Figure 1 indicates the case when $k > 1$. If the gas molecule type is the same, since the excitation function F is the same, even if the molecular number density N differs, the value of electron energy, where the radiation intensity becomes maximum, should be the same. In other words, for the I-curve at $N = N_1$, the I-curve when $N = kN_1$ would be the one obtained by multiplying the reference I-curve multiplied by k times in the direction of the abscissa.

What would happen to Fig. 1 if the abscissa were the electric field E? Although it is hard to know beforehand the electron energy in actual experiments, the electric field E may be easily found from $E = V/L$. Here, V is the voltage, and L is the distance between the electrodes. The mean electron energy in field E may be expressed by the following equation[3]:

$$W \propto E/N \tag{2}$$

If the mean electron energy in the electric field, where the radiation intensity reaches a maximum, is W_1, and the electric field, where the mean electron energy becomes W_1 when the gas molecular number density is N_1, is E_1, the following equation may be established:

$$W_1 \propto E_1/N_1 = kE_1/kN_1 \tag{3}$$

This equation means the following: When the molecular number density N_1 increases by k times to kN_1, the radiation intensity becomes maximum when the electric field increases to kE_1. The same becomes true not only at the maximum point on the I-curve, but at all positions on the I-curve. Therefore, for the curve in Fig. 1, if the abscissa is the electric field E, when the molecular number density of the gas increases by k times to kN, the I-curve for the molecular number density kN would be the curve in which the point on the I-curve at molecular number density N is shifted by k times in the direction of the abscissa, and is multiplied by k times in the direction of the ordinate.

Now, for the radiation from the electric discharge column which crosses the shock wave, the radiation intensity from the discharge column in the freestream, where the molecular number density is N_∞, is I_∞; and that from the discharge column in the shock wave layer, where the molecular number density is Ns, is Is. Since we can assume $N_\infty = N_1$ and $Ns = kN_1$ by selecting a suitable value of k, for the reasons explained above, the I_∞-curve and Is-curve from two regions may be roughly expressed as shown in Fig. 2. In this case, it may be accepted that the electric field is more or less equal in two regions, one in the freestream and the other in the shock-wave layer which are close enough to the shock wave. Therefore, the relationship between I_∞ and Is regarding the change in the electric field E may be described as follows: The figure shows that I_∞ is larger than Is when the electric field E is small enough. I_∞ and Is become equal at the electric field value where the two curves cross. We cannot visualize the shock position in this case. Moreover, if the electric field becomes larger than the value, Is becomes larger than the I_∞. From the relations described above, the radiation intensity ratio I_∞/Is vs the electric field E is briefly obtained as shown in Fig. 2. Figure 2 shows that the value of I_∞/Is becomes minimum at a certain value of E. The reason for the occurrence of this

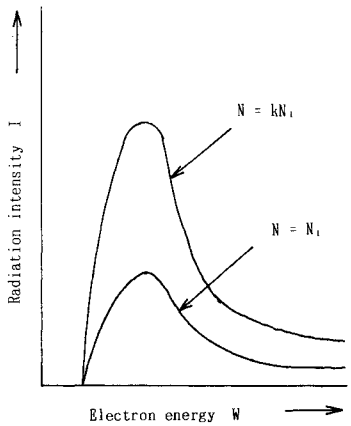

Fig. 1 Radiation intensity curves vs electron energies in case that molecular number density is parameter.

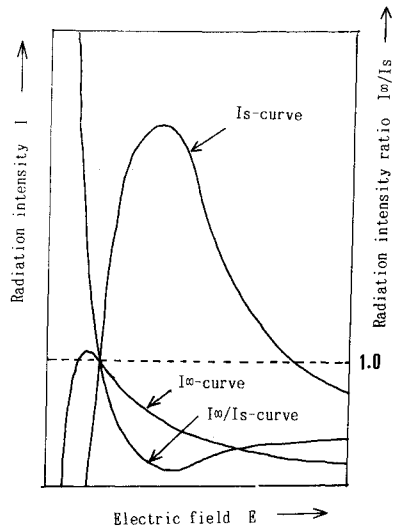

Fig. 2 Radiation intensity curves from two regions: one in the freestream and the other in the shock layer (radiation intensity ratio I_∞/Is).

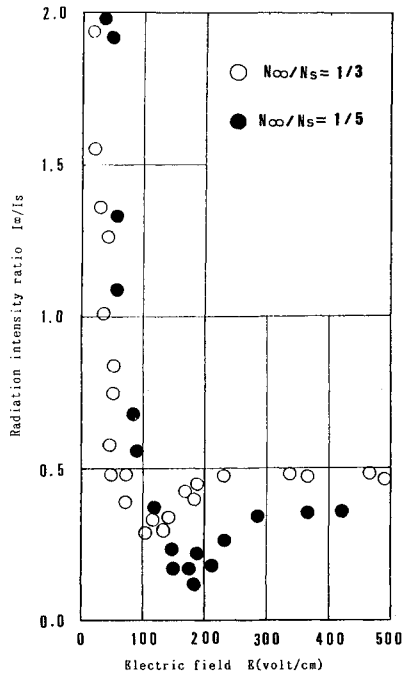

Fig. 3 Relation between radiation intensity ratio I_∞/Is and electric field E obtained experimentally.

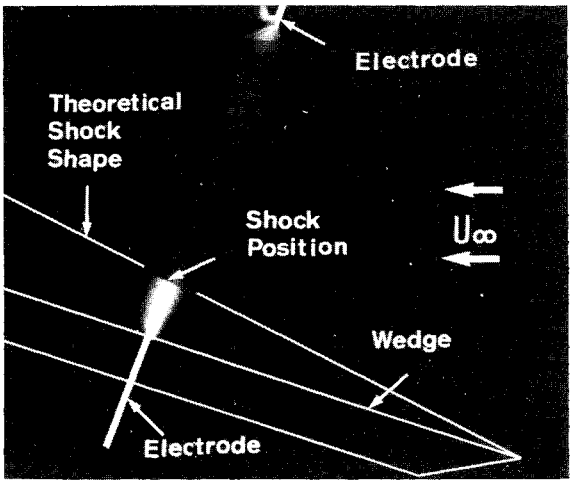

Fig. 4 Visualization of shock position over a wedge model.

minimum value is the decline of excitation functions after reaching the maximums, as mentioned before.

To verify the correctness of the above qualitative predictions, the relation between the value of the radiation intensity ratio I_∞/Is and the electric field E were investigated experimentally. In these experiments, shock waves were generated over a wedge. Electric discharges which cross the shock waves were generated under various electric fields and the electric discharge columns were photographed. From these discharge photographs, the radiation intensities I_∞ and Is at both parts just before and behind the shock waves were read with a sensitometer. Then, the radiation intensity ratio I_∞/Is was obtained. To read the radiation intensities at these parts of the discharge columns, a calibration curve was made in advance. The calibration curve was made as follows. The known intensities of light were applied to the films. The relative sensitization degree of these films was read with the sensitometer. Therefore, the relative radiation intensities from these parts of the discharge columns were obtainable by reading the sensitization degree at these parts with the sensitometer. These experiments were carried out when the molecular number density ratio N_∞/Ns was 1/3 and 1/5 by changing the angle of attack of the wedge. In these experiments, N_∞ was about 10^{17}/cm. The experimental results are shown in Fig. 3. It is shown that the qualitatively predicted I_∞/Is-curve vs the electric field agrees considerably with the results obtained experimentally.

In the case of $I_\infty/Is = 1$, the shock shape cannot be visualized since there exists no radiation contrast at the shock position. When the electric field is small enough, it seems to be suitable for the visualization of shock shapes since $I_\infty/Is \gg 1$ is realized. However, in order to generate an electric discharge under the condition of a small electric field, a great amount of electric current is required. Consequently, the flowfield would be disturbed and the visualization of shock shapes would not be successful. Therefore, it is best to select the electric field value at which the value of I_∞/Is is minimum.

The visualization of a shock wave generated over a wedge is demonstrated in Fig. 4. The characteristics of the hypersonic tunnel used in this experiment were as follows: Mach number is 10, static pressure is 1 mm Hg, flow duration is 10^{-2} s, and the diameter of the hypersonic nozzle exit is 0.15 m. The type of gas is air. The molecular number densities in the freestream and shock-wave layer are about $10^{17}/cm^3$ and $4.7 \times 10^{17}/cm^3$, respectively. A Nikon F camera is set just outside the observation window. The camera is set open during the experiment, and therefore the exposure time of the film is equivalent to the duration of the electric discharge itself. The film speed is ASA 1600. An electric discharge is generated while the hypersonic flow is obtained. The electric field in this experiment is about 150 V/cm. Concerning this electric discharge, the radiation intensity ratio I_∞/Is is about 1/5. The result indicates that the shock position is visualized exactly and clearly. The electric discharge can be photographed not only from the side, but also from the rear. Therefore, the present method can visualize three-dimensional shock shapes.

References

[1]Kimura, T., and Nishio, M., "Visualization of Shock Wave by Electric Discharge," *AIAA Journal*, Vol. 15, No. 5, 1977, pp. 611-612.

[2]Nasser, E., *Fundamentals of Gaseous Ionization and Plasma Electronics*, Wiley-Interscience, New York, 1970, pp. 74-75.

[3]Engel, V., *Ionized Gases*, Oxford Univ. Press, Oxford, England, UK, 1965, pp. 122-123.

Decoupling Approximation of Nonclassically Damped Structures

Steven Park,* Ilwhan Park,* and Fai Ma†
University of California, Berkeley,
Berkeley, California 94720

I. Introduction

In the analysis of a linear dynamic system, it is common practice to express the equations of motion in modal coordinates. If the resulting modal damping matrix is not diagonal, the system is said to be nonclassically damped. Because the existence of off-diagonal terms in the modal damping matrix complicates the analysis, the off-diagonal terms are usually ignored. This procedure is called the decoupling approximation. However, the off-diagonal terms can have significant influence on the response of a system, and ignoring the off-diagonal terms may cause substantial errors. An attempt to derive error bounds for the decoupling approximation has recently been reported by Shahruz and Ma[1] and by Hwang and Ma.[2] The purpose of this study is to present an exact analytical formula for the error and to illuminate the parameters that must be considered before the decoupling approximation can be applied to the equations of motion. For nonclassically damped linear systems subjected to harmonic excitations, three parameters in the equations of motion must be taken into consideration. The three parameters consist of the modal damping matrix, the natural frequencies, and the external excitation. The modal damping matrix and the natural frequencies are already known to be influential parameters, and their effect on the approximation error has been examined. We show in this Note that it is not adequate to consider just these two parameters. The interplay between all three parameters can lead to significant errors when invoking the decoupling approximation. Therefore, a proper study of the applicability of the decoupling approximation should include all three parameters.

A specific decoupling criterion based on just two parameters, the modal damping matrix and the natural frequencies, has been defined by Hasselman[3] and also by Warburton and Soni.[4] The criterion depends specifically on the amount of frequency separation between two natural frequencies, and it was asserted that adequate frequency separation between the modes is a sufficient condition for ignoring the off-diagonal terms of the modal damping matrix. It will be shown in this paper that frequency separation is not sufficient in insuring

Received June 4, 1991; revision received Jan. 17, 1992; accepted for publication Jan. 18, 1992.

*Research Assistant, Department of Mechanical Engineering.

†Associate Professor of Applied Mechanics, Department of Mechanical Engineering.